The EMBO Journal (2013) 32, 2950–2962
www.embojournal.org

TRANSPARENT PROCESS

THE EMBO JOURNAL

Structural basis for the MukB-topoisomerase IV interaction and its functional implications *in vivo*

Seychelle M Vos[1], Nichole K Stewart[2], Martha G Oakley[2] and James M Berger[1,3,*]

[1]Department of Molecular and Cell Biology, University of California, Berkeley, CA, USA and [2]Department of Chemistry, Indiana University, Bloomington, IN, USA

Chromosome partitioning in *Escherichia coli* is assisted by two interacting proteins, topoisomerase (topo) IV and MukB. MukB stimulates the relaxation of negative supercoils by topo IV; to understand the mechanism of their action and to define this functional interplay, we determined the crystal structure of a minimal MukB–topo IV complex to 2.3 Å resolution. The structure shows that the so-called 'hinge' region of MukB forms a heterotetrameric assembly with a C-terminal DNA binding domain (CTD) on topo IV's ParC subunit. Biochemical studies show that the hinge stimulates topo IV by competing for a site on the CTD that normally represses activity on negatively supercoiled DNA, while complementation tests using mutants implicated in the interaction reveal that the cellular dependency on topo IV derives from a joint need for both strand passage and MukB binding. Interestingly, the configuration of the MukB•topo IV complex sterically disfavours intradimeric interactions, indicating that the proteins may form oligomeric arrays with one another, and suggesting a framework by which MukB and topo IV may collaborate during daughter chromosome disentanglement.

The EMBO Journal (2013) **32,** 2950–2962. doi:10.1038/emboj.2013.218; Published online 4 October 2013
Subject Categories: genome stability & dynamics; structural biology
Keywords: chromosome segregation; chromosome condensation; structural maintenance of chromosomes (SMCs); topoisomerase

Introduction

Appropriate coordination of DNA replication and chromosome segregation is critical to the maintenance of genetic integrity (Kato *et al*, 1988; Hartwell and Weinert, 1989; Hiraga *et al*, 1989; Weinert *et al*, 1994; Uhlmann and Nasmyth, 1998). In bacteria, replication and chromosome partitioning occur concurrently as a means to apportion progeny with the proper amount of genetic material (Viollier *et al*, 2004; Bates and Kleckner, 2005; Nielsen *et al*, 2006; Wang *et al*, 2006b; Joshi *et al*, 2011). During replication and segregation, cellular machineries must confront certain physical challenges that arise from DNA's inherently long, intertwined structure. For example, replisome progression generates positive supercoils in front of the advancing fork, as well as precatenanes between newly replicated sisters (Hiasa and Marians, 1996; Peter *et al*, 1998; Sogo *et al*, 1999; Khodursky *et al*, 2000; Postow *et al*, 2001a). Failure to adequately remove replication-dependent supercoils and precatenanes can have significant consequences for the cell, resulting in incomplete DNA replication and improper DNA segregation (Kato *et al*, 1990; Sogo *et al*, 1999; Postow *et al*, 2001b; Hardy *et al*, 2004; Bermejo *et al*, 2007; Baxter and Diffley, 2008; Fachinetti *et al*, 2010). Deficiencies in chromosome condensation similarly can produce cells with segregation defects, resulting in a high percentage of anucleate cells (Kato *et al*, 1990; Niki *et al*, 1991; Graumann, 2000; Wang *et al*, 2006a; Hirano, 2012).

In Eubacteria, multiple factors aid with accurate condensation and partitioning (Boles *et al*, 1990; Hardy *et al*, 2004; Luijsterburg *et al*, 2008). For example, supercoiling allows close packing of DNA helices that reduces chromosomal volume (Boles *et al*, 1990; Postow *et al*, 2004). Proteinaceous factors such as nucleoid-associated proteins (NAPs), topoisomerases, and structural maintenance of chromosomes (SMCs) proteins play a similarly key role (Hardy *et al*, 2004; Luijsterburg *et al*, 2008). In *E. coli*, topoisomerase (topo) IV uses an ATP-dependent DNA breakage, passage, and rejoining mechanism to resolve both positive supercoils and catenated DNA structures (Kato *et al*, 1990; Peng and Marians, 1993a,b; Zechiedrich and Cozzarelli, 1995; Hiasa and Marians, 1996; Khodursky *et al*, 2000). The *E. coli* SMC homologue, MukB, likewise can affect topological transformations in DNA, primarily by altering DNA writhe (Petrushenko *et al*, 2006a; Cui *et al*, 2008).

Recent studies have shown that MukB and topo IV interact physically and that MukB can stimulate the ability of topo IV to relax negatively supercoiled DNA (Hayama and Marians, 2010; Li *et al*, 2010b; Hayama *et al*, 2013). On its own, topo IV operates as a heterotetramer containing two copies of ParE, the ATPase subunit of the enzyme, and two copies of ParC, which binds and cleaves DNA (Kato *et al*, 1990, 1992; Peng and Marians, 1993b). By comparison, MukB consists of two globular domains—an ABC-ATPase 'head' region and an internal 'hinge' element—linked by 50 nm long antiparallel coiled-coil arms (Melby *et al*, 1998; Ku *et al*, 2009; Woo *et al*, 2009; Li *et al*, 2010a). The interaction between MukB and topo IV has been mapped to the MukB hinge (Li *et al*, 2010b), which can form a stable dimer (Li *et al*, 2009, 2010a), and the ParC C-terminal domain (CTD) (Hayama and Marians, 2010; Li *et al*, 2010b), which is monomeric when liberated from its associated N-terminal region (Corbett *et al*, 2005) (Figure 1A). At present, the mechanism by which MukB alters topo IV activity, along with the physical interactions

*Corresponding author. Department of Molecular and Cell Biology, California Institute of Quantitative Biosciences, University of California at Berkeley, 374D Stanley Hall, Berkeley, CA 94720, USA.
Tel.: +1 510 643 9483; Fax: +1 510 666 2768;
E-mail: jmberger@jhmi.edu
[3]Present address: Department of Biophysics and Biophysical Chemistry, Johns Hopkins University School of Medicine, 725North Wolfe Street, WBSB 713, Baltimore, MD 21205, USA

Received: 20 May 2013; accepted: 11 September 2013; published online: 4 October 2013

©2013 European Molecular Biology Organization

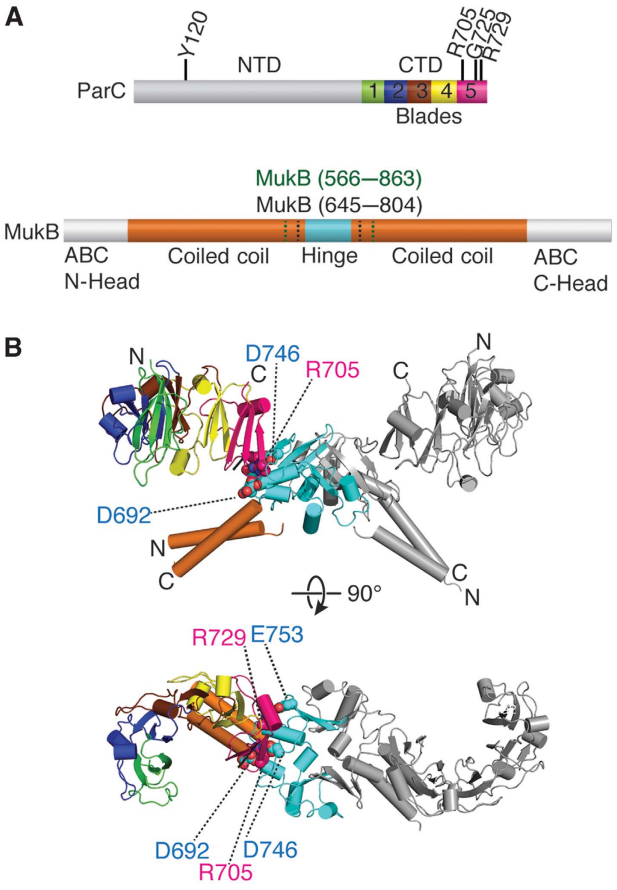

Figure 1 Structure of a MukB hinge•topo IV complex. (**A**) Primary structure and domain organization of *E. coli* ParC and MukB. A subset of the ParC residues addressed in this study are labelled on the primary structure. MukB hinge constructs (aa 566–863 (green), aa 645–804 (black)) used here are also denoted. Different subdomain repeats of the CTD (termed as 'blades') are coloured rainbow. (**B**) Crystal structure of the hinge CTD heterotetramer in cartoon representation. Colouring for one MukB hinge and ParC CTD is as per (**A**), with dimer-related protomer coloured grey. Residues mutated and assayed in this study are depicted as spheres and labelled.

that promote complex formation, has not been established. The extent to which topo IV's association with MukB, as opposed to its strand-passage activity, helps support cell viability is similarly unclear.

To better understand the nature and functional consequences of the MukB–topo IV interaction, we determined the crystal structure of the MukB hinge in complex with the ParC CTD. The structure shows that the CTD and the hinge form a symmetric complex in which a negatively charged outer surface of MukB associates with a positively charged patch on the perimeter of the CTD. We find that the hinge alone can specifically stimulate topo IV activity on negatively supercoiled substrates, and that this stimulation arises through competition for a strong DNA-binding surface on the CTD that otherwise represses the relaxation of negatively supercoiled DNA. Curiously, the structure of the complex reveals that the mutation responsible for thermal sensitivity in *E. coli* C600*parc1215* cells maps to the surface of the CTD occupied by MukB; complementation studies establish that the strand-passage and MukB-binding functions of topo IV are independent but additive activities that work together to promote cell growth. Geometric considerations of the structure obtained here suggest that topo IV and MukB can assemble into oligomeric arrays, the formation of which may be useful for resolving newly replicated daughter chromosomes.

Results and Discussion

Structural characterization of MukB–ParC interaction

To identify a minimal interaction complex between topo IV and MukB for crystallographic studies, we cloned, purified, and performed pull-down assays with various hinge constructs and the isolated ParC CTD (497–752). The CTD bound to all hinge variants tested, but did not associate with the Ni^{2+} beads or with the coiled-coil arms alone, indicating that the ParC CTD binds directly to the globular core of the hinge region (not shown). The smallest hinge construct identified by this approach (residues 645–804, corresponding to a fragment previously analysed crystallographically; Ku *et al*, 2009) was subsequently used for structural studies.

For screening crystallization conditions, the minimized MukB hinge and the ParC CTD were individually overexpressed and purified from *E. coli*, and then mixed immediately before setting trays. Co-crystals grew in the space group $P2_12_12_1$ and diffracted to 2.3 Å resolution. The structure was solved using a combination of molecular replacement and single-wavelength anomalous dispersion for phasing (Figures 1B and 2A). The final model, which includes residues 497/498–742 of ParC and residues 645–801/804 of MukB, was refined to an R_{work}/R_{free} of 20.4%/24.6% and shows good stereochemistry (Table I, Materials and methods).

Previous studies of the MukB•ParC interaction indicated that two ParC CTDs could bind a single dimer of the MukB hinge (Li *et al*, 2010b). This binding stoichiometry is recapitulated in the asymmetric unit of the hinge•CTD co-crystals, which contains a single heterotetrameric complex (Figure 1B). The *E. coli* ParC CTD adopts a crescent-shaped structure composed of five repeating Greek-key folds, or 'blades' (Figure 1). In our structure, the fifth blade of the CTD—the element furthest from the N-terminus of the region—interacts with the hinge. The interface between the hinge and the CTD is small, burying a total surface area of ~690 Å^2 per protomer. The residues mediating the interaction lie predominantly on loops that connect adjoining secondary structural elements (Figure 2A), and are highly conserved only in γ-proteobacterial MukB and ParC orthologues (Supplementary Figure S1). Surface electrostatic-potential maps show that the negatively charged hinge of MukB associates with a portion of the positively charged strip that encircles the outer surface of the ParC CTD (Figure 2B); these interactions are responsible for the majority of the contacts between the two domains. In particular, a positively charged string of residues on the CTD comprising residues Lys704, Arg705, and Lys706 interacts with Glu688/Asp691, Asp692/Asp746, and Asp745, respectively, on MukB. Two additional sets of ionic interactions in the structure include crosstalk between Asp692 of MukB and Arg733 of ParC, and between Arg729 of the CTD and hinge residues Glu696, Asp697, and Glu753. Only one hydrophobic residue, Phe701 of MukB, participates in the hinge-CTD interface, where it

©2013 European Molecular Biology Organization

Table I Data collection, refinement, and stereochemistry statistics

Data collection	Remote	Peak
Resolution (Å)	49.97–2.3	50–3.1
Wavelength (Å)	1.1	0.979648
Space group	P212121	P212121
Unit cell dimensions (*a*, *b*, *c*) (Å)	49.76, 103.67, 186.59	49.713, 103.633, 186.537
Unit cell angles (α, β, γ) (deg)	90, 90, 90	90, 90, 90
I/σ (last shell)	17.0 (2.78)	15.0 (4.68)
R_{merge} (last shell) (%)	6.2 (39.4)	12.2 (34.2)
Completeness (last shell) (%)	98.1 (88.5)	99.3 (100)
Redundancy	3.8 (2.8)	4.3 (4.3)
Unique reflections	44 001	18 525
Number of sites		18
Fig of merit		0.37
Refinement		
Resolution (Å)	49.974–2.3	
No. of reflections	43 079	
R_{work} (%) (last shell)	20.4 (25.4)	
R_{free} (%) (last shell)	24.6 (31.5)	
Structure and stereochemistry		
No. of atoms	6684	
Protein	6335	
Water	349	
B factor (Å^2)		
Protein	20.0	
Water	33.5	
R.m.s.d. bond lengths (Å)	0.002	
R.m.s.d. bond angles (deg)	0.552	
Ramachandran plot (%)		
Favoured region	98.1	
Allowed region	1.7	
Outliers	0.1	

$R_{merge} = \Sigma_{hkl} | I_i(hkl) - \langle I(hkl) \rangle | / \Sigma_{hkl} I_i(hkl)$, where $I_i(hkl)$ is the intensity of an observation and $\langle I(hkl) \rangle$ the mean value for its unique reflection. Summations cover all reflections.
$R_{work} = \Sigma_{hkl} | F_{obs} - k \cdot F_{calc} | / \Sigma_{hkl} F_{obs}$. R_{free} was as per R_{work}, but with the reflections excluded from refinement. The R_{free} set was chosen using default parameters in PHENIX (Adams *et al*, 2010).
Ramachandran plot categories were defined by MolProbity (Chen *et al*, 2010).

is coordinated by cation-pi interactions with Arg705 and Arg729 of ParC.

Residues in the MukB•ParC interface are necessary for mutual interactions

The structure of the hinge•CTD complex accounts for previous mutagenesis efforts implicating Glu688, Asp692, Asp697, Asp745, and Glu753 of MukB, and Arg705 and Arg729 of ParC, in the interaction of the two proteins (Hayama and Marians, 2010; Li *et al*, 2010b; Hayama *et al*, 2013). To further probe the contacts seen in the structure, we designed, purified, and performed pull-down assays using other mutations that map to the MukB•ParC interface (Supplementary Figures S2–S3). In these experiments, a CTD construct bearing an N-terminal, His_6-MBP tag was incubated with Ni^{2+} beads in the presence or absence of the core region of the hinge that bears a portion of the coiled-coil arms (residues 566–863). The wild-type hinge associated with the MBP-tagged CTD but did not associate with the Ni^{2+} beads (Supplementary Figure S3A). A CTD double mutant, Arg705Asp/Arg729Asp (which resembles a previously characterized CTD mutant, Arg705Glu/Arg729Ala; Hayama and Marians, 2010), likewise behaved as expected, failing to pull-down the MukB hinge. Similarly to the MukB Asp692Ala mutation studied previously (Li *et al*, 2010b), a more severe single point mutant in the hinge, Asp692Phe, still only partially abrogated the interaction with the CTD (Supplementary Figure S3B); however, when two additional MukB mutations were added to this substitution (Asp746Arg and Glu753Arg, which should disrupt interactions with residues Arg705, Arg729, and Arg733 of ParC), the hinge completely failed to associate with the MBP-tagged CTD. Together with the original mutagenesis studies (Hayama and Marians, 2010; Li *et al*, 2010b; Hayama *et al*, 2013), these data confirm that the residues implicated by our crystal structure are essential for forming the MukB•ParC binding interface.

MukB antagonizes DNA binding by the ParC CTD

The ParC CTD is a DNA-binding domain that helps topo IV to differentiate between positively and negatively supercoiled substrates (Corbett *et al*, 2005; Vos *et al*, 2013). The region of the CTD responsible for these activities has been postulated to rely on a positively charged strip that encircles the CTD (Figure 2B) (Corbett *et al*, 2005; Vos *et al*, 2013). The isolated CTD of ParC has been shown to bind duplex DNA somewhat modestly, with an apparent dissociation constant of $\sim$1 μM (Corbett *et al*, 2004). Because the structure of the complex reported here shows that MukB binds to the outer surface of the ParC CTD, we reasoned that its effect on the activity of topo IV activity could arise by an ability to modulate DNA binding by the ParC CTD directly.

In a recent study (Vos *et al*, 2013), we found that the behaviour of the isolated ParC CTD, which is prone to aggregate over time, could be improved by leaving the domain fused to the MBP tag used for expression and our pull-down assays. To determine how well the MBP-tagged CTD binds DNA, we carried out fluorescence anisotropy experiments using a fluorescein-labelled 20mer duplex oligonucleotide (Figure 3A). This analysis showed that the MBP-ParC CTD construct binds DNA with an apparent affinity similar to that reported previously for the isolated domain ($K_{d,app} \cong$ 1–2 μM) (Corbett *et al*, 2004). Hence, the MBP fusion does not appear to compromise DNA binding in and of itself.

We next tested whether MukB affects DNA binding by the ParC CTD. Unlike other SMCs, whose hinges can associate with both single- and double-stranded DNA (Chiu *et al*, 2004; Hirano and Hirano, 2002, 2006; Griese and Hopfner, 2010; Griese *et al*, 2010), MukB binds DNA with its ABC-ATPase head domain but not with its hinge (Ku *et al*, 2009; Woo *et al*, 2009; Li *et al*, 2010a; Hayama *et al*, 2013). Consistent with these data, no association was observed by fluorescence anisotropy when the hinge was incubated with the 20mer duplex DNA in the absence of the CTD (Supplementary Figure S4A). By contrast, the presence of the hinge significantly reduced DNA binding by the MBP-tagged CTD in the same assay (Figure 3A). To confirm these results, we performed surface plasmon resonance experiments using a sensor chip coated with a biotinylated 20mer oligonucleotide of identical sequence to the one used in the fluorescence anisotropy experiments. DNA was pre-bound with the MBP-ParC CTD construct and then washed with solutions

 ©2013 European Molecular Biology Organization

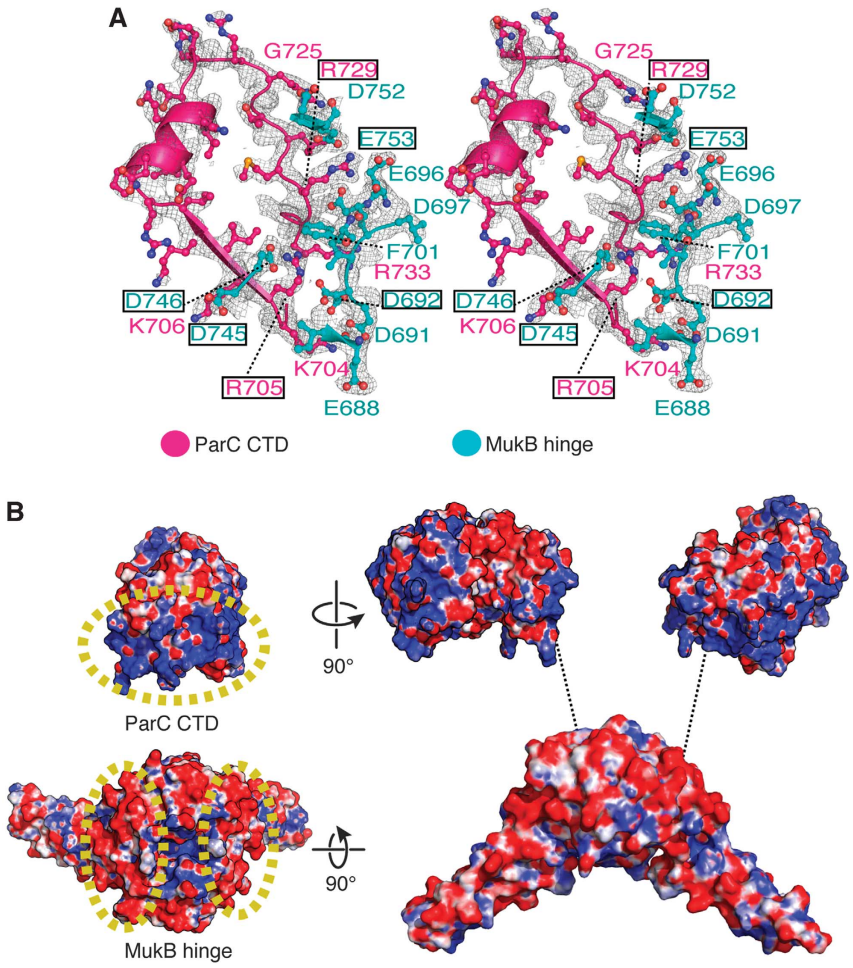

Figure 2 The hinge•CTD interaction is predominantly electrostatic. (**A**) Stereo representation of MukB hinge (cyan)•ParC CTD (pink) interface shown with a $2F_o - F_c$ map contoured at 1σ. Interacting residues are labelled; boxed residues were mutated and assayed in this study. (**B**) Electrostatic potential map of the MukB•ParC interaction surfaces. On the left, a single ParC CTD and MukB hinge dimer are coloured according to surface charge (blue for positive and red for negative). The interacting surfaces of MukB and ParC are demarcated by yellow, dashed ovals. On the right, an exploded view of the hinge-CTD complex is shown.

containing a constant concentration of the MBP-ParC CTD (250 nM) and various amounts of the MukB hinge. Addition of the MukB hinge resulted in a decrease in response units in a dose-dependent manner (Figure 3B), suggesting that as with the fluorescence anisotropy results, the MukB hinge competes directly with DNA for binding the ParC CTD.

We next tested whether our MukB hinge mutants could interfere with DNA binding by the CTD. Similar to results obtained for the wild-type hinge, we found that a hinge construct containing the single Asp692Phe substitution, which only weakens the interaction between the two proteins, modestly diminished DNA binding by the CTD (Figure 3A). By contrast, the triply substituted hinge (Asp692Phe/Asp746Arg/Glu753Arg), which does not bind to the CTD, did not interfere appreciably with the CTD–DNA association (Figure 3A). Interestingly, while conducting these studies, we unexpectedly found that the Arg705Asp/Arg729Asp double substitution in the CTD, which maps to the MukB-binding site on ParC, is severely compromised for binding DNA, even when MukB is absent (Figure 3C). In context of the topo IV holoenzyme, the Arg705Asp/Arg729Asp double substitution has a negligible effect on the overall binding of a 42-mer duplex oligonucleotide (~2-fold decrease in binding affinity; Supplementary Figure S4C), consistent with recent work indicating that this region of the CTD transiently associates with T-segment DNA (Corbett *et al*, 2005; Vos *et al*, 2013). Overall, our results reveal that the MukB-binding interface overlaps with a strong DNA-binding site on the ParC CTD, and that the MukB hinge specifically competes with DNA by associating with this surface.

To determine whether the MukB hinge blocks DNA from binding to the CTD of ParC in particular, we next performed fluorescence anisotropy experiments using a dye-labeled duplex and the analogous C-terminal region from the *E. coli* paralogue of topo IV, gyrase. The construct chosen for this work (residues 531–853 of the corresponding GyrA subunit) lacks an autoinhibitory C-terminal tail (Tretter and Berger, 2012), thereby permitting the domain to robustly bind and wrap DNA on its own (Reece and Maxwell, 1991; Ruthenburg *et al*, 2005; Tretter and Berger, 2012). When the GyrA CTD (531–853) was incubated with the hinge, we observed little effect on DNA binding (Figure 3D; Supplementary Figure S4B, $K_{d,app} > 100\,\mu M$). This result demonstrates that the

©2013 European Molecular Biology Organization

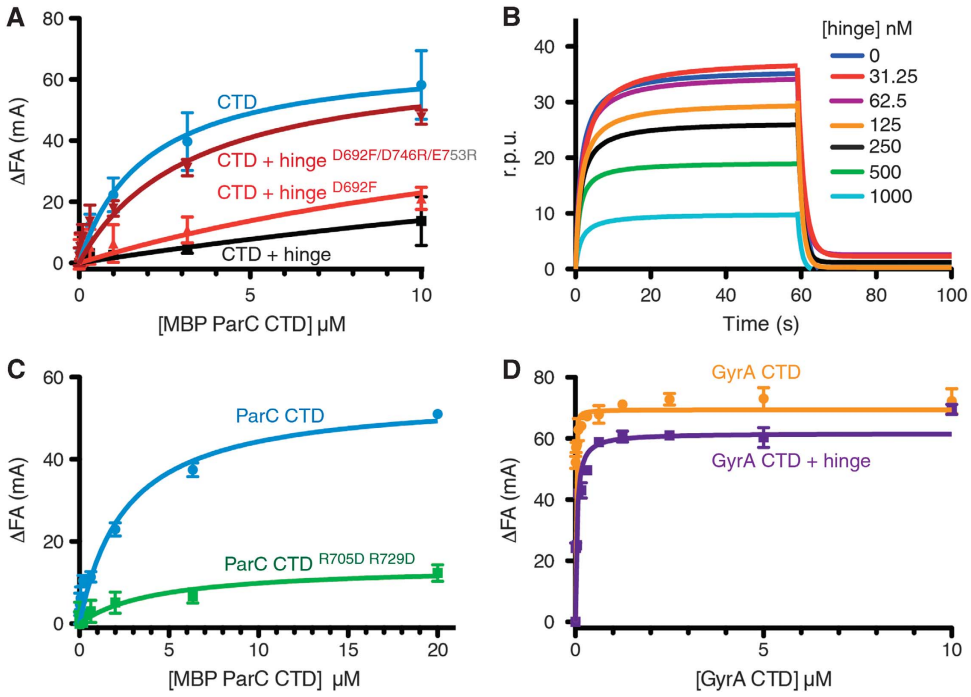

Figure 3 The hinge prevents the ParC, but not the GyrA CTD from binding DNA. (**A**) Binding of the MBP-ParC CTD to 20 nM of a fluorescently labelled 20mer duplex oligonucleotide (20 nM), as monitored by relative change (ΔFA) in fluorescence anisotropy (millianisotropy units—mA). Data correspond to titrations with MBP-ParC CTD (CTD) alone, or with 10 μM of the WT MukB hinge, the Asp692Phe mutant, or the Asp692Phe/Asp746Arg/Glu753Arg mutant. See also Supplementary Figure S4. (**B**) DNA binding by the MBP-tagged CTD as monitored by surface plasmon resonance in the presence of different hinge concentrations. The y axis indicates changes in response units (r.p.u.) due to protein association with the DNA bound sensor chip. The DNA substrate is identical in sequence to the DNA substrate utilized in the fluorescence anisotropy experiments. (**C**) DNA binding by the MBP-ParC CTD$^{R705D/R729D}$ mutant as determined by fluorescence anisotropy. Substrate is the same as in (**A**). (**D**) DNA binding by the tailless *E. coli* GyrA CTD (aa 531–853) construct as determined by fluorescence anisotropy in the presence and absence of the MukB hinge (10 μM). Substrate is the same as in (**A**). See also Supplementary Figure S4.

MukB hinge is specific for blocking DNA binding by the ParC CTD and not for impeding binding by bacterial type IIA topoisomerase CTDs in general.

The MukB hinge stimulates topo IV activity on negatively supercoiled DNA

It has recently been observed that full-length MukB specifically stimulates the ability of topo IV to relax negatively supercoiled, but not positively supercoiled, plasmid substrates (Hayama *et al*, 2013). Full-length MukB is known to independently alter DNA supercoiling and condensation (Petrushenko *et al*, 2006a; Chen *et al*, 2008; Cui *et al*, 2008), and it has been suggested that MukB stimulates topo IV's activity, at least in part, by altering the topological state of the DNA through which both proteins associate. Evidence for this idea has derived from the observation that a MukB mutant, which can no longer associate with DNA through its head regions, fails to enhance the relaxation of negatively supercoiled plasmid substrates by topo IV (Hayama *et al*, 2013). However, it has also been found that the isolated MukB hinge, which lacks DNA-binding activity, can stimulate negative-supercoil relaxation (Li *et al*, 2010b). This latter result has been interpreted as evidence that MukB might alter topo IV's activity directly.

To better distinguish how MukB impacts topo IV function, we used our structure and collection of mutants to reinvestigate the effects of the isolated MukB hinge on the wild-type topo IV holoenzyme. In designing these studies, we recognized that the MukB•ParC interaction is weak ($K_d \cong 0.5$ μM) compared to the relative dissociation constants of topo IV and MukB for supercoiled DNA (which are low to subnanomolar) (Charvin *et al*, 2005; Petrushenko *et al*, 2006a; Li *et al*, 2010b); because of this difference, we reasoned that DNA might facilitate the co-association of MukB and topo IV at low protein concentrations, and that in the absence of DNA (or if MukB is unable to bind DNA), higher concentrations would be needed to promote complex formation. To ensure efficient complex formation, positive- and negative-supercoil relaxation experiments were therefore performed in the presence of topo IV and different amounts of the MukB hinge using a topoisomerase concentration (500 nM) near the observed K_d for the hinge•CTD interaction. Since topo IV rapidly catalyses strand-passage events (~2–3/s) (Charvin *et al*, 2003; Stone *et al*, 2003), and is ~20-fold more active on positively supercoiled substrates than on negatively supercoiled substrates (Crisona *et al*, 2000; Charvin *et al*, 2003; Stone *et al*, 2003; Neuman *et al*, 2009), both high plasmid concentrations and low temperature were used to slow down the reactions so that experiments conducted in the absence of MukB would only partially go to completion within a measureable timeframe.

In analysing DNA topoisomers, native-agarose gel electrophoresis is frequently employed to resolve slowly migrating relaxed plasmid molecules from more rapidly moving supercoiled species. When the products of the topo IV/MukB hinge reactions were monitored by this approach, we found that the

 ©2013 European Molecular Biology Organization

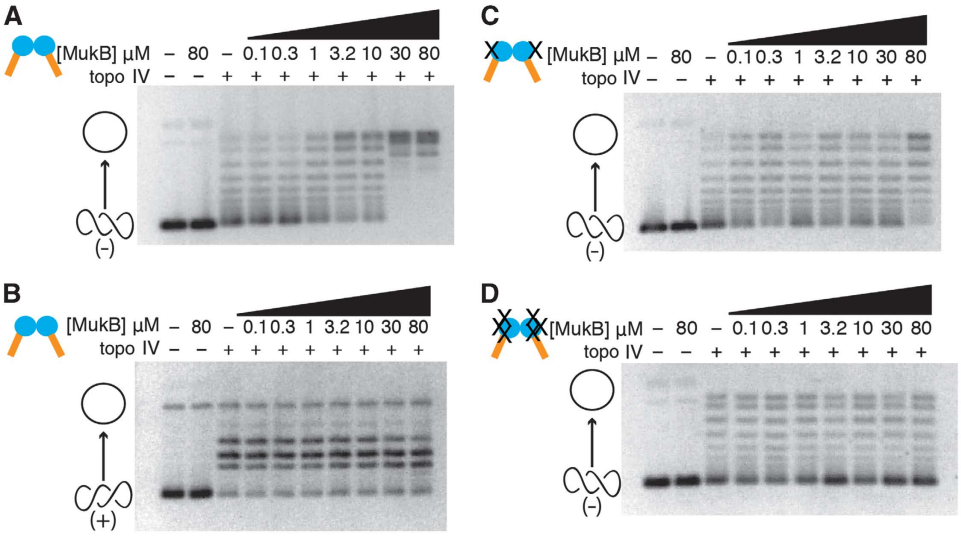

Figure 4 The hinge activates topo IV on negatively supercoiled but not on positively supercoiled DNA. All panels show the relaxation of supercoiled pSG483 plasmid substrate by an equimolar amount of topo IV (500 nM). Negatively supercoiled substrates were used for (**A**, **C**, and **D**). (**B**) The results for positively supercoiled substrate are shown. In each instance, reactions were quenched midway to prevent full relaxation of the DNA by topo IV alone, so as to determine any effects of MukB (see Supplementary Figure S5 for the corresponding activity time course). Different panels compare different MukB hinge constructs: (**A**, **B**) WT MukB hinge; (**C**) Asp692Phe hinge mutant; (**D**) AspD692Phe/AspD746Arg/Asp753Arg hinge mutant. Cartoon representations of topoisomer states are shown on the left side of the gels (open circle—relaxed species; intertwined circles—supercoiled species).

isolated hinge domain was able to stimulate the relaxation of negatively supercoiled DNA, with stimulation starting at near-stoichiometric ratios of topo IV and increasing as a function of hinge concentration in a dose-dependent manner (Figure 4A). Interestingly, the hinge did not stimulate the relaxation of positively supercoiled DNA by topo IV (Figure 4B; Supplementary Figure S5). This result indicates that the effect of the hinge on topo IV activity is specific for the handedness of the DNA substrate, a behaviour recently reported by Marians and co-workers for full-length MukB (Hayama *et al*, 2013).

To investigate whether the stimulatory action of the hinge depended on the contacts seen in the crystal structure, we next performed topo IV relaxation experiments using our collection of MukB and ParC interface mutants. We found that the single MukB^{D692F} hinge mutant weakly stimulated topo IV activity, and only at high molar excess (i.e., 160-fold or greater than topo IV) (Figure 4C). By contrast, the triple MukB$^{D692F/D746R/E753R}$ hinge mutant (which does not associate with the CTD; Supplementary Figure S3) failed to stimulate the relaxation of negatively supercoiled substrates at any of the measured concentrations (Figure 4D). Together, these data support the proposal that binding of the MukB hinge to the ParC CTD can directly and specifically fine-tune the activity of topo IV on negatively supercoiled DNA.

Because MukB appears to compete for a strong DNA-binding surface on the CTD (Figure 3C), the effect of the hinge on topo IV suggested that the activity of the topoisomerase might be naturally repressed on negatively supercoiled substrates. To test this idea, we examined the concentration-dependent and time-dependent activity of the ParC Arg705Asp/Arg729Asp double mutant compared to the wild-type enzyme. Analysis of the resultant data shows that the activity of the ParC CTD double mutant is elevated with respect to the native enzyme on negatively supercoiled DNA (Figure 5A), but that these substitutions have no effect on topo IV function with positively supercoiled substrates (Figure 5B). Interestingly, the extent to which the ParC mutations increase the rate of supercoil relaxation approximates the modest degree of stimulation promoted by the MukB hinge alone (~1.5- to 2-fold; Figure 5C). These results are consistent with recent findings from our laboratory showing that different surfaces of the topo IV CTD contribute non-equivalently to the relaxation of positively and negatively supercoiled DNAs (Vos *et al*, 2013), and indicate that the MukB hinge exerts its topology-specific effects on topo IV function by binding to and masking an auto-repressive region.

The strand-passage and MukB-binding functions of topo IV serve distinct but additive roles in the cell

E. coli parC is an essential gene that was discovered in a screen for temperature-sensitive mutants that improperly partitioned sister chromosomes (*E. coli* C600*parC1215*) (Kato *et al*, 1988, 1990). The temperature sensitivity of the *E. coli* C600*parC1215* strain generally has been attributed to the loss of topo IV decatenation activity at the restrictive temperature (Zechiedrich and Cozzarelli, 1995; Nurse *et al*, 2003; Perez-Cheeks *et al*, 2012). However, during the course of our studies, we realized that the mutation responsible for the thermosensitivity of the *E. coli* C600*parC1215* strain, Gly725Asp (Kato *et al*, 1990), not only resides in the ParC CTD, but actually lies between two residues that bind MukB in our crystal structure (Arg705 and Arg729) (Figure 2A).

Because Gly725 does not map to a region of topo IV responsible for strand passage, the severe phenotypic consequences arising from its mutation to aspartate raised the question as to whether the topo IV–MukB interaction might play a separable but additive role with the cell's need for a potent DNA decatenase. To test this idea, we used complementation assays to interrogate the activity of topo IV mutations that would be expected to selectively com-

©2013 European Molecular Biology Organization

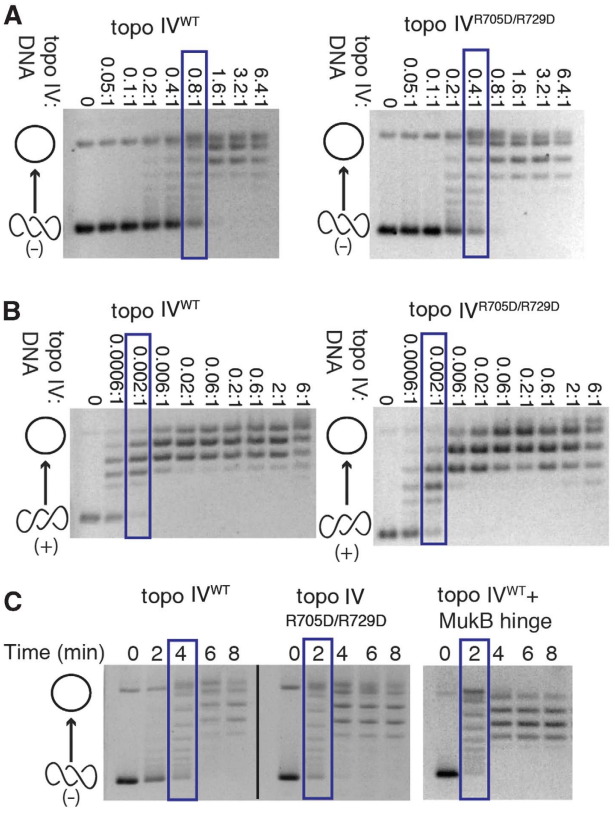

Figure 5 The hinge masks a DNA-binding site on the CTD that autorepresses the relaxation of negatively supercoiled DNA. Native gels show the relaxation of either negatively or positively supercoiled pSG483 plasmid substrates by WT topo IV or by Arg705Asp/Arg729Asp topo IV (which does not bind MukB). Cartoon representations of topoisomer states are shown on the left side of the gels (open circle—relaxed species and intertwined circles—supercoiled species). Blue boxes indicate protein concentration or time point at which topo IV has relaxed approximately half the supercoiled substrate. Gels are representative of at least three independent replicates from three different protein topo IV preparations. (**A**) Enzyme titrations showing that mutation of the MukB-binding site on the ParC CTD leads to elevated relaxation activity on negatively supercoiled DNA. The molar ratio of enzyme:DNA is indicated above each gel (reactions contained 7.9 nM supercoiled plasmid). (**B**) Enzyme titrations showing that mutation of the MukB-binding site on the ParC CTD does not affect the relaxation of positively supercoiled DNA. The molar ratio of enzyme:DNA is indicated above each gel (reactions contained 7.9 nM supercoiled plasmid). (**C**) Rates of negative-supercoil relaxation are similarly stimulated by either the Arg705Asp/Arg729Asp ParC mutation or binding of the MukB hinge. Reactions contain 500 nM of plasmid DNA and 500 nM of either WT or mutant topo IV (500 nM), together with the presence or absence of 10 μM of the MukB hinge.

promise strand passage, MukB binding, or both. *E. coli* C600*parC1215* cells were first grown at 30°C to mid-log phase, and then shifted to the restrictive temperature (42°C). Aliquots were removed at various time points after the shift, serially diluted (20-fold steps), and plated on both rich and minimal media; this scheme allowed us to first impose conditions of fast and slow growth, and to then assess the extent to which cells adapted to the restrictive temperature before plating. C600*parC1215* cells bearing a control plasmid encoding the wild-type $parC^{+}$ gene were fully competent at both the permissive (30°C) and restrictive temperatures (42°C) on both types of growth media (Figure 6; Supplementary Figure S6). Conversely, cells transformed with the empty vector control were able to grow only at the permissive temperature and showed no ability to adapt to non-permissive conditions. Together, these data show that the vectors and conditions used for the assay work as shown previously (Lavasani and Hiasa, 2001; Perez-Cheeks *et al*, 2012), and establish upper and lower limits on the extent of growth seen under complementing and non-complementing conditions.

We next assessed the ability of three different topo IV constructs to complement the C600*parC1215* strain, starting first with cells plated on rich media (Figure 6A; Supplementary Figure S6A). When transformed with a plasmid expressing the $parC^{Y120F}$ allele, which ablates both the catalytic tyrosine and strand-passage function of topo IV, cells showed diminished growth at the restrictive temperature, but were nonetheless viable. The $parC^{R705D/R729D}$ allele, which contains a disrupted MukB-binding locus, but does not impede topo IV relaxation activity, was also able to partially complement growth at 42°C. By contrast, when provided with a plasmid that could express only the ParC N-terminal domain (NTD), a construct that both lacks the MukB-binding site entirely and that exhibits only 2–5% of the specific activity of wild-type topo IV (Corbett *et al*, 2005), cells responded as if they had been transformed with an empty vector, showing an essentially complete loss of growth at the restrictive temperature. Interestingly, when exposed to short, liquid-culture incubations for progressively longer periods of time, cells harbouring either the $parC^{Y120F}$ or $parC^{R705D/R729D}$ genes (but not the $parC^{NTD}$ gene) began to lose their temperature sensitivity; sequencing confirmed that neither the plasmids nor the chromosomal loci had reverted in these cells (Supplementary Figure S6). Similar phenotypic effects were seen when cells were grown on minimal media (Figure 6B; Supplementary Figure S6B), although the $parC^{R705D/R729D}$ allele proved more able to complement the temperature-sensitive strain, a result consistent with prior observations showing that MukB is not required for viability when cells are grown under slowly proliferative conditions (Niki *et al*, 1991; Champion and Higgins, 2007).

Together, the ParC CTD appears to be required for overall cell viability. Moreover, while the MukB•ParC interaction is not essential in a strict sense, it aids the fitness of rapidly growing cells in a manner that is additive with a need for robust strand-passage activity by topo IV. On the basis of the available biochemical data provided here and by others (Hayama and Marians, 2010; Hayama *et al*, 2013), it seems likely that an inability to interact with MukB underlies the effect of the Arg705Asp/Arg729Asp CTD mutant *in vivo*. This information, together with the observed partial complementation conferred by the $parC^{Y120F}$ gene, in turn suggests that the mutant ParC protein is particularly defective in the C600*parC1215* strain because of a global stability defect in its CTD that leads to both a loss of MukB binding and a diminution of topoisomerase activity. Consistent with this hypothesis, attempts to purify a Gly725Asp ParC mutant have proven to be unsuccessful due to low expression and aggregation of the protein.

Prospective role of the topo IV•MukB interaction in vivo

Given its role as a key decatenase in *E. coli*, the finding that the strand-passage activity *per se* of topo IV is not absolutely essential for cell viability may seem at first surprising.

©2013 European Molecular Biology Organization

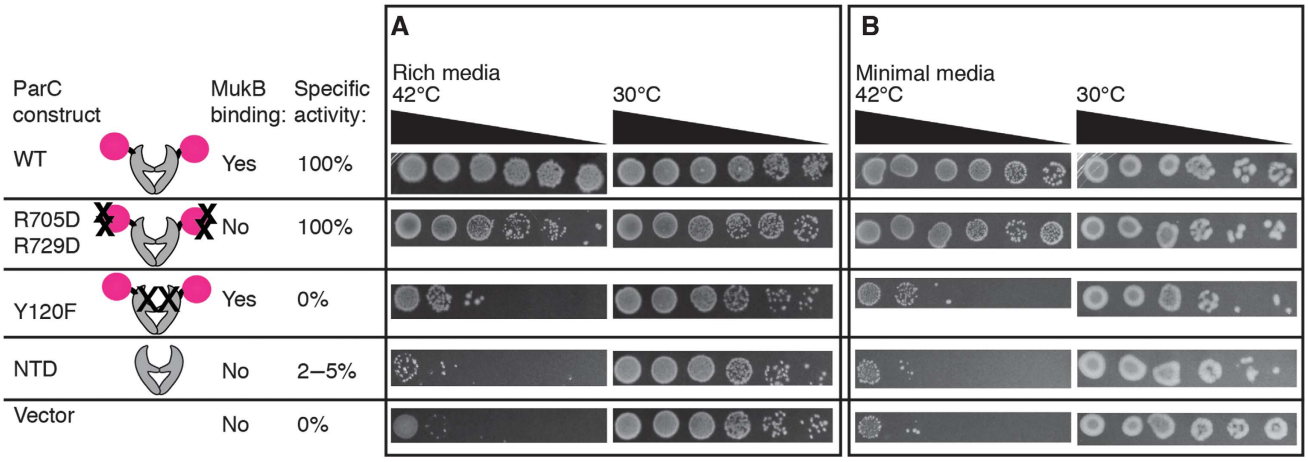

Figure 6 The strand-passage activity of topo IV and its ability to bind MukB are separable and contribute additively to cell growth. Complementation assays of the *C600parc1215* strain are shown grown at 42°C on rich (**A**) and minimal (**B**) media. Spotted cultures correspond to 20-fold dilution series taken 1 h after liquid cultures were shifted to the restrictive temperature. For plating, cells were normalized to the culture with the lowest OD_{600nm} at the time of the temperature shift ($OD_{600nm} \approx 0.3$). Cartoons of ParC constructs assayed, their specific activity relative to WT, and their ability to bind MukB, are illustrated next to each row. Dilutions of cells grown at the permissive temperature (30°C) are shown to the right of cells grown at the restrictive temperature. Time points taken from cultures at time points 30–270 min after the temperature shift are shown in Supplementary Figure S6.

However, other topoisomerases, notably gyrase and topo III, can compensate for loss of topo IV *in vivo*. For example, overexpression of either topo III, a type IA topoisomerase capable of unlinking hemicatenanes (DiGate and Marians, 1988; Hiasa *et al*, 1994), or gyrase, a type IIA topoisomerase that negatively supercoils DNA (Gellert *et al*, 1976), can complement *parC* or *parE* temperature-sensitive strains (Kato *et al*, 1992; Zechiedrich and Cozzarelli, 1995; Nurse *et al*, 2003; Lopez *et al*, 2005; Perez-Cheeks *et al*, 2012). By contrast, loss of topo III in the C600*parC1215* temperature-sensitive strain results in severe chromosome segregation defects and a near-complete loss of viability at 25°C, whereas conjoining a Δ*top3* allele with a *parE* temperature-sensitive strain gives rise to cells that exhibit segregation defects at 30°C but are nonetheless capable of growth (Perez-Cheeks *et al*, 2012). These results suggest that, in addition to its ability to remove catenanes, the ability of ParC to specifically interact with MukB is one of the essential roles of topo IV. It may be that the phenotype exhibited by the $parE^{ts}$ Δ*top3* strain is less severely compromised because cells still retain the ability to form a ParC•MukB complex even though they have lost their primary decatenase.

If the topo IV•MukB interaction is important to the cell, then what purpose might it serve? MukB and topo IV are independently required for the appropriate segregation of sister chromosomes during and after DNA replication (Niki *et al*, 1991; Badrinarayanan *et al*, 2012a; Wang *et al*, 2008), but are not required to complete replicative strand synthesis *per se* (Kato *et al*, 1990; Niki *et al*, 1991; Danilova *et al*, 2007; Wang *et al*, 2008). The localization of topo IV to precatenanes is thought to aid in the rapid removal of the linkages between newly replicated DNA strands (Wang *et al*, 2008); however, additional interactions between the enzyme and MukB could facilitate this process further. In this vein, it is instructive to consider the architecture of what a fully intact topo IV•MukB complex might look like (Figure 7B). A typical type IIA topoisomerase holoenzyme is in the order of ∼150–200 Å in size (Kirchhausen *et al*, 1985; Baker *et al*, 2011; Schmidt *et al*, 2012; Papillon *et al*, 2013). By comparison, a MukB homodimer forms an extended structure of ∼500 Å long (Melby *et al*, 1998). Interestingly, docking of the full-length *E. coli* ParC subunits onto a MukB hinge dimer, using the CTDs to guide placement, shows that the spacing of the CTDs on the hinge is too close to permit a single MukB homodimer to simultaneously bind both subunits of a ParC dimer (Figure 7A). Although the CTD is probably able to change position relative to the central DNA-binding channel, it is unclear whether the domain can undergo the extensive movements required to bind MukB in a 2:2 stoichiometry. Moreover, if two CTDs could attain the requisite geometry, then their resultant position would occlude the binding sites for G-segment DNA and ParE on ParC, preventing the formation of a catalytically active topo IV holoenzyme. By contrast, the observed positions of the CTD on topo IV can permit co-assembly with MukB to create higher order chains of the two proteins (Figure 7B). In such a scheme, were separate MukB•topo IV oligomers to preferentially localize on each of the two sisters, topo IV would be in a position to specifically resolve the links between sisters, thereby favouring appropriate chromosome segregation into daughter cells (Figure 7C).

Several lines of evidence are consistent with an array type of model. During the initial stages of replication in *E. coli*, sister chromosomes remain associated at the cell centre (Sunako *et al*, 2001; Bates and Kleckner, 2005; Reyes-Lamothe *et al*, 2008; Wang *et al*, 2008). After this early phase of cohesion, sister chromosomes move apart, with the *oriC* of each sister relocating to either one-fourth or three-fourth positions of the cell (Bates and Kleckner, 2005; Nielsen *et al*, 2006; Reyes-Lamothe *et al*, 2008; Joshi *et al*, 2011). Sister cohesion has been proposed to be mediated by the precatenanes formed between the newly replicated sisters, as a slight overexpression of topo IV drastically reduces the period of sister cohesion (Wang *et al*, 2008; Lesterlin *et al*, 2012). In context of a MukB•topo IV oligomer model, the two proteins may associate to ensure that MukB can properly localize to precatenanes during the initial phases of DNA replication, where it subsequently

©2013 European Molecular Biology Organization

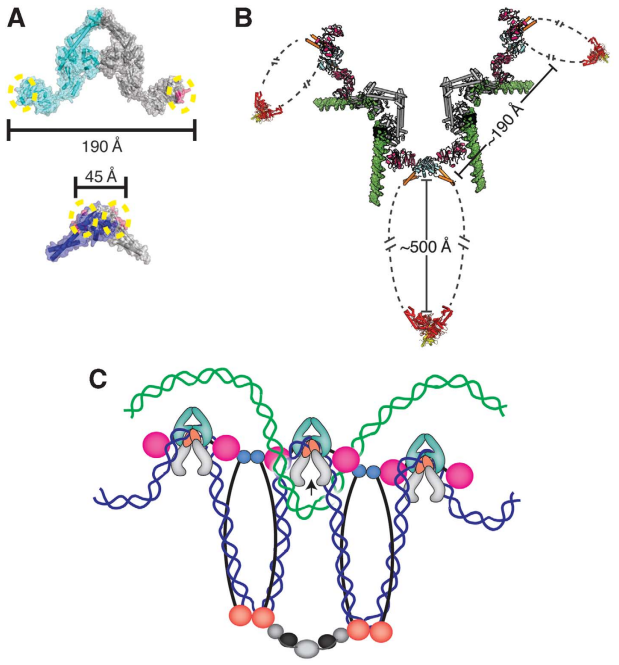

Figure 7 Physical considerations for the formation of higher order MukB•ParC oligomers. (**A**) The geometry of the MukB•topo IV interaction does not favour intradimeric complex formation. *Upper*—MukB-binding sites (magenta with dotted yellow circles) are marked on the crystal structure of the *E. coli* ParC dimer (cyan and grey) (PDB ID: IZVU). *Lower*—The ParC-binding sites (magenta with dotted yellow circles) are marked on the crystal structure of the *E. coli* MukB hinge dimer (navy blue and grey) (PDB ID: 3IBP). The distances between binding sites are shown in Ångströms. (**B**) The geometry of the MukB•topo IV interaction permits formation of oligomeric arrays. The ParC CTD (pink)•MukB hinge (cyan) coiled-coil arms (orange) structure determined here is shown docked onto with the full-length *E. coli* ParC crystal structure (grey) (PDB ID: IZVU), modelled with a docked G-segment DNA (green) (superposed from PDB ID: 2RGR). For perspective, the *Haemophilus ducreyi* MukB head domain (red) in complex with MukF (yellow) (PDB ID: 3EUJ) is also shown. Distances between subunits and domains are labelled. (**C**) One prospective functional role of a MukB•ParC oligomeric array. Oligomers of MukB and ParC form through the hinge (cyan)•CTD (pink) interaction; MukB oligomers are further stabilized by interactions of their head domains with accessory proteins, MukE (black) and MukF (grey). If MukB and ParC engage the same newly replicated sister chromosome (blue) through DNA bending and looping, then the array predisposes topo IV to remove catenated crossovers formed with the corresponding sister chromosome (green).

assists in dragging DNA to the one-fourth and three-fourth positions by an as yet unknown mechanism.

If ParC and MukB are prelocalized to precatenanes generated in the wake of a replication fork, then why are these regions not immediately unlinked? Interestingly, ParC is reported to be at least two times more abundant in cells than ParE, suggesting that only a subset of ParC is associated with ParE in topo IV heterotetramers (Taniguchi *et al*, 2010; Wang *et al*, 2012). ParC and ParE have also been reported to localize to different regions of the cell (Huang *et al*, 1998; Espeli *et al*, 2003; Wang and Shapiro, 2004), and have been proposed to come together at specific times to form an active complex competent for removing supercoils and catenanes. Were such a separation of function to occur, it could make a prospective topo IV•MukB array competent to segregate daughters only at specific points during replication. Consistent with this idea, overexpression of topo IV is toxic and results in both segregation and locus partitioning defects (Wang *et al*, 2008; Lesterlin *et al*, 2012). Since MukB and the ParC subunit of topo IV are expressed at similar levels in cells (Taniguchi *et al*, 2010; Badrinarayanan *et al*, 2012b; Wang *et al*, 2012), overexpression of ParC could also disrupt topo IV•MukB chains, thus impeding appropriate chromosome partitioning. Such a mechanism would parallel that proposed for MukE and MukF, which have been suggested to partition MukB between oligomeric $(B_2E_2F)_n$ chains and single $B_2E_4F_4$ complexes depending on the relative stoichiometries of the three proteins (Wang *et al*, 2006a; Petrushenko *et al*, 2006b, 2010; She *et al*, 2007; Badrinarayanan *et al*, 2012b). In this regard, MukE and MukF, which specially link MukB head domains together (Woo *et al*, 2009; Badrinarayanan *et al*, 2012b), could provide a stabilizing anchor to a topo IV•MukB assembly, which would occur through the hinge on the opposite side of the condensin.

One feature of the action of MukB on topo IV not immediately apparent from this model is why the hinge should specifically stimulate negative-supercoil relaxation by topo IV. Interestingly, attempts to abrogate this stimulation—either by using a large molar excess of the hinge or by using hinge heterodimers containing only a single functional ParC-binding site (Figure 4A; Supplementary Figure S7)—were unsuccessful, indicating that the prospective formation of MukB•topo IV oligomers is not responsible for the observed activation. Recent data from our group have shown that distinct surfaces of the ParC CTD contribute differentially to relaxation of supercoiled DNA substrates and the resolution of catenanes (Vos *et al*, 2013). One potential reason MukB may bind to the fifth blade of the ParC CTD is because alterations to this region do not impair the enzymatic activity of topo IV; as such, the stimulatory effects observed *in vitro* may simply be a fortuitous byproduct of the interaction. Alternatively, during rapid DNA replication, MukB could stimulate topo IV to specifically remove negative supercoils that form behind the replisome in the leading sister strand (supercoils cannot form in the lagging strand due to the gaps between the Okazaki fragments) (Supplementary Figure S8). Future studies will be required to determine whether large-scale MukB•topo IV oligomers do indeed form on DNA and how such complexes might help facilitate daughter chromosome disentanglement and appropriate partitioning.

Materials and methods

Cloning of MukB and ParC constructs for crystallography and biochemistry

Cloning of the ParC CTD (497–752), full-length ParC (1–752), full-length ParE (1–630), the ParC NTD (1–482)(Corbett *et al*, 2005), the His_6-MBP-ParC CTD (Vos *et al*, 2013), and MukB (645–804) have been described previously (Li *et al*, 2010b). Mutations were made by QuikChange (Agilent).

Protein expression and purification

Protein expression and purification for all constructs is described in detail in Supplementary Methods. Briefly, all proteins were overexpressed as His_6 or His_6-MBP fusion proteins in *E. coli*, using BL21codon-plus (DE3) RIL cells (Stratagene) and either IPTG or autoinduction procedures. Selenomethoinine labelling, where used, was carried out using the method of Van Duyne *et al* (1993). Following lysis by sonication, proteins were purified by a

 ©2013 European Molecular Biology Organization

combination of affinity chromatography, proteolysis to remove the fusion tags, and size-exclusion chromatography. Purified samples were concentrated, dialysed, and either flash-frozen or used immediately for subsequent studies.

Crystallography and data collection

For crystallography, the selenomethionine-labelled ParC CTD (residues 487–752) and MukB hinge (residues 645–804) were dialysed separately at 15–20 mg/ml concentration each for 16 h at 4°C against 100 mM KCl, 20 mM Tris–HCl pH 7.9, and 0.5 mM TCEP. The hinge and CTD were then mixed at equimolar ratios immediately before setting trays. Crystals were grown at 18°C in hanging drop format by combining 1 μl of well solution (212.5 mM lithium citrate tribasic tetrahydrate, 20% PEG 3350) with 1 μl of the hinge/CTD mix. Crystals generally formed within 24 h and were cryoprotected by adding a solution containing the protein buffer, well solution, and 30% PEG 400 directly to the drop. After cryoprotection, the crystals were immediately looped and flash frozen in liquid nitrogen.

Diffraction data sets (two remote and two peak) were collected from a single crystal at Beamline 8.3.1 at the Advanced Light Source at Lawrence Berkeley National Laboratory (MacDowell *et al*, 2004). Data were indexed and scaled with ELVES and HKL2000, revealing that the unit cell belongs to the space group $P2_12_12_1$ (Otwinowski and Minor, 1997; Holton and Alber, 2004). Phase calculations were performed with PHENIX AutoSOL (Terwilliger *et al*, 2009), using a combination of single-wavelength anomalous dispersion and molecular replacement with the ParC CTD (PDB ID 1ZVT) the MukB hinge (PDB ID 3IBP) as search models. Manual building was performed with COOT (Emsley *et al*, 2010) and the complete hinge•CTD heterotetramer model refined with PHENIX (Adams *et al*, 2010). TLS parameters were analysed by the TLSMD server, which generated 24 groups for use in the late stages of refinement (Painter and Merritt, 2006). The final model was refined to an R_{work}/R_{free} of 20.4%/24.6%, with Molprobibity analysis showing that 98.5% of residues reside in favoured Ramachandran space and one residue occupies a disallowed region (0.13%) (Chen *et al*, 2010). The atomic structure and coordinate files have been deposited with the Protein Data Bank (ID 4MN4). Figures were prepared with PyMol (DeLano, 2002).

DNA-binding assays

A randomly generated, 20 bp annealed duplex oligonucleotide (5′-|56-FAM|-TTAGGCGTAAACCTCCATGC-3′ and 5′-AATCCGCATT TGGAGGTACG-3′, where |56-FAM| indicates the position of a carboxyfluorescein dye used for analysis) was purchased from Integrated DNA Technologies (IDT) and resuspended in water (50% G/C content, $T_m = 50$°C). All proteins were diluted on ice in protein dilution buffer (300 mM potassium glutamate, 20 mM Tris–HCl pH 7.5, 10% glycerol, and 0.05 mg/ml bovine serum albumin (BSA)). The assay contained 4 μl of the His_6-MBP ParC CTD (0.01–10 μM) mixed with either 4 μl of the MukB hinge (aa 566–863, 10 μM) or 4 μl of protein dilution buffer and 20 nM of the fluorescently labelled 20mer oligonucleotide. DNA and proteins were initially incubated on ice in the dark for 10 min, after which they were diluted to the final assay volume (80 μl) and kept at room temperature in the dark for 10 min (final assay conditions: 2.4 mM DTT, 20 mM Tris–HCl pH 7.5, 10% (v/v) glycerol, 1 mM $MgCl_2$, 0.05 mg/ml BSA, 30 mM potassium glutamate). Measurements were made with a Perkin Elmer Victor 3V 1420 multilabel plate reader at 535 nm. Data points are the average of three independent experiments and all points are normalized to wells that did not contain protein. Data were plotted in GraphPad Prism Version 5 using the following single-site binding equation:

$$y = B_{max}\left(\frac{([x]+[L]+K_{d,app}) - \sqrt{([x]+[L]+K_{d,app})^2 - 4([x]\bullet[L])}}{2\bullet[L]}\right)$$

where B_{max} is the maximum specific binding, L is the DNA concentration, x is the His_6-MBP ParC CTD concentration, and $K_{d,app}$ is the apparent dissociation constant for His_6-MBP ParC CTD and DNA (Kenakin, 1993; Swillens, 1995; Lundblad *et al*, 1996). DNA-binding experiments with the *E. coli* GyrA CTD (531–853) were performed in an identical manner to those described for the His_6-MBP ParC CTD. Surface plasmon resonance experiments are described in Supplementary Methods.

Preparation of supercoiled plasmid substrates

Negatively supercoiled pSG483 (2927 bp), a pBlueScript SK derivative, was prepared from *E. coli* using a maxiprep kit (Machery-Nagel). To produce positively supercoiled pSG483, negatively supercoiled pSG483 was treated with *A. fulgidus* reverse gyrase following the method of Rodriguez (2002). Plasmid DNAs were concentrated to 6–10 mg/ml by speed-vac.

DNA supercoil relaxation assays

Supercoil relaxation assays are described in detail in Supplementary Methods. Briefly, topo IV heterotetramers were formed by adding equimolar ParE and ParC to a final concentration of 40 μM in dilution buffer. Topo IV was incubated with MukB (566–863) and supercoiled pSG483 plasmid DNA (500 nM final concentration) at either 25°C (for negative-supercoil relaxation) or 15°C (for positive-supercoil relaxation) in a solution containing 30 mM potassium glutamate, 1% (v/v) glycerol, 10 mM DTT, 1 mM spermidine, 10 μg/ml BSA, 50 mM Tris–HCl pH 7.9, 6 mM $MgCl_2$, and 2 mM ATP pH 7.5. Samples were removed and quenched at various time points (15 s to 10 min) with stop buffer (100 mM EDTA, 10% SDS (w/v)). Samples were then diluted and run for 6–18 h on 1% (w/v) TAE agarose gels (40 mM sodium acetate, 50 mM Tris–HCl pH 7.9, 1 mM EDTA pH 8.0) at 2–2.5 volts/cm. To visualize the DNA, gels were stained with 0.5 μg/ml ethidium bromide in TAE buffer for 20 min, destained in TAE buffer for 30 min, and exposed to UV transillumination. Assays of topo IV-specific activity were carried out as per Vos *et al* (2013), and were performed at least three times with three different enzyme preparations.

Temperature-sensitive complementation assays

The C600*ParC1215* strain was a generous gift of Hiroshi Hiasa (Kato *et al*, 1988, 1990; Lavasani and Hiasa, 2001). ParC constructs were cloned into a modified pET28b vector with a ligation-independent cloning site (Doyle, 2005). The C600*ParC1215* strain was complemented by leaky expression from T7 promoter containing rescue plasmids as previously described (Lavasani and Hiasa, 2001) (Supplementary Methods). Cells were transformed and plated on 2xYT or M9 minimal media supplemented with 2% (w/v) glucose (Sambrook and Russell, 2001) and grown at 30°C. M9 minimal media was made with M9 salts, 0.2% (v/v) glucose, 1 mM $MgSO_4$ 1 μg/ml thiamine, 116.75 mg/l threonine, 58.25 mg/l leucine, and 100 μM $CaCl_2$. Several colonies were picked to start 5 ml overnight liquid cultures grown in 2% (w/v) glucose. Overnight cultures were then used to inoculate duplicate 50 ml liquid cultures containing either 2xYT or M9 minimal media and incubated at 30°C. When cells reached an OD_{600} of 0.3 ± 0.05, duplicate liquid media cultures were split so that one remained at the permissive temperature (30°C) while the other was shifted to the non-permissive temperature (42°C). Cells were adapted to the new temperature for 30 min, after which cells were grown for an additional 4 h with time points taken at 30, 60, 150, and 270 min post temperature shift. Cells were serially diluted after normalization, plated, and grown at 30°C and 42°C to assess survival resulting from leaky expression for each time point. For all plating dilutions, cells were normalized to the culture with the lowest OD_{600} at the 0-min time point. Additional details for these experiments are provided in Supplementary Methods.

Supplementary data

Supplementary data are available at *The EMBO Journal* Online (http://www.embojournal.org).

Acknowledgements

We thank George Meigs and James Holton for assistance with crystallography at Advanced Light Source Beamline 8.3.1; Berger Lab members, including Allyn Schoeffler and Nathan Thomsen, for assistance with crystallography, and Richard Rymer and Karl Duderstat for biochemical advice; Deborah Thurtle of the Rine Lab (UC Berkeley) and Qingrong Yan of the Kuriyan Lab (UC Berkeley) for advice and the use of equipment in conducting the complementation assays and surface plasmon resonance studies,

©2013 European Molecular Biology Organization

respectively; and Reviewer 2 for the suggestion that MukB might help topo IV remove negative supercoils formed on the newly replicated leading strand. This work was supported by a National Science Foundation Pre-doctoral fellowship to SMV, Indiana University (MGO) and the NCI (R01-CA077373 to JMB).

Author contributions: SMV, NKS, MGO, and JMB designed the research. SMV conducted all of the experiments and worked with JMB in analysing and interpreting the data. SMV, NKS, and MGO contributed reagents. SMV and JMB wrote the manuscript with input from NKS and MGO.

References

Adams PD, Afonine PV, Bunkoczi G, Chen VB, Davis IW, Echols N, Headd JJ, Hung LW, Kapral GJ, Grosse-Kunstleve RW, McCoy AJ, Moriarty NW, Oeffner R, Read RJ, Richardson DC, Richardson JS, Terwilliger TC, Zwart PH (2010) PHENIX: a comprehensive Python-based system for macromolecular structure solution. *Acta Crystallogr D Biol Crystallogr* 66: 213–221

Badrinarayanan A, Lesterlin C, Reyes-Lamothe R, Sherratt D (2012a) The Escherichia coli SMC complex, MukBEF, shapes nucleoid organization independently of DNA replication. *J Bacteriol* **194:** 4669–4676

Badrinarayanan A, Reyes-Lamothe R, Uphoff S, Leake MC, Sherratt DJ (2012b) *In vivo* architecture and action of bacterial structural maintenance of chromosome proteins. *Science* **338:** 528–531

Baker NM, Weigand S, Maar-Mathias S, Mondragon A (2011) Solution structures of DNA-bound gyrase. *Nucleic Acids Res* **39:** 755–766

Bates D, Kleckner N (2005) Chromosome and replisome dynamics in E. coli: loss of sister cohesion triggers global chromosome movement and mediates chromosome segregation. *Cell* **121:** 899–911

Baxter J, Diffley JFX (2008) Topoisomerase II inactivation prevents the completion of DNA replication in budding yeast. *Mol Cell* **30:** 790–802

Bermejo R, Doksani Y, Capra T, Katou YM, Tanaka H, Shirahige K, Foiani M (2007) Top1- and Top2-mediated topological transitions at replication forks ensure fork progression and stability and prevent DNA damage checkpoint activation. *Genes Dev* **21:** 1921–1936

Boles TC, White JH, Cozzarelli NR (1990) Structure of plectonemically supercoiled DNA. *J Mol Biol* **213:** 931–951

Champion K, Higgins NP (2007) Growth rate toxicity phenotypes and homeostatic supercoil control differentiate Escherichia coli from Salmonella enterica serovar Typhimurium. *J Bacteriol* **189:** 5839–5849

Charvin G, Bensimon D, Croquette V (2003) Single-molecule study of DNA unlinking by eukaryotic and prokaryotic type-II topoisomerases. *Proc Natl Acad Sci USA* **100:** 9820–9825

Charvin G, Strick TR, Bensimon D, Croquette V (2005) Topoisomerase IV bends and overtwists DNA upon binding. *Biophys J* **89:** 384–392

Chen N, Zinchenko AA, Yoshikawa Y, Araki S, Adachi S, Yamazoe M, Hiraga S, Yoshikawa K (2008) ATP-induced shrinkage of DNA with MukB protein and the MukBEF complex of Escherichia coli. *J Bacteriol* **190:** 3731–3737

Chen VB, Arendall 3rd WB, Headd JJ, Keedy DA, Immormino RM, Kapral GJ, Murray LW, Richardson JS, Richardson DC (2010) MolProbity: all-atom structure validation for macromolecular crystallography. *Acta Crystallogr D Biol Crystallogr* **66:** 12–21

Chiu A, Revenkova E, Jessberger R (2004) DNA interaction and dimerization of eukaryotic SMC hinge domains. *J Biol Chem* **279:** 26233–26242

Corbett KD, Schoeffler AJ, Thomsen ND, Berger JM (2005) The structural basis for substrate specificity in DNA topoisomerase IV. *J Mol Biol* **351:** 545–561

Corbett KD, Shultzaberger RK, Berger JM (2004) The C-terminal domain of DNA gyrase A adopts a DNA-bending beta-pinwheel fold. *Proc Natl Acad Sci USA* **101:** 7293–7298

Crisona NJ, Strick TR, Bensimon D, Croquette V, Cozzarelli NR (2000) Preferential relaxation of positively supercoiled DNA by E. coli topoisomerase IV in single-molecule and ensemble measurements. *Genes Dev* **14:** 2881–2892

Cui Y, Petrushenko ZM, Rybenkov VV (2008) MukB acts as a macromolecular clamp in DNA condensation. *Nat Struct Mol Biol* **15:** 411–418

Danilova O, Reyes-Lamothe R, Pinskaya M, Sherratt D, Possoz C (2007) MukB colocalizes with the oriC region and is required for organization of the two Escherichia coli chromosome arms into separate cell halves. *Mol Microbiol* **65:** 1485–1492

DeLano WL (2002; The PyMOL Molecular Graphics System(http://www.pymol.org)

DiGate RJ, Marians KJ (1988) Identification of a potent decatenating enzyme from *Escherichia coli*. *J Biol Chem* **263:** 13366–13373

Doyle SA (2005) High-throughput cloning for proteomics research. *Methods Mol Biol* **310:** 107–113

Emsley P, Lohkamp B, Scott WG, Cowtan K (2010) Features and development of Coot. *Acta Crystallogr D Biol Crystallogr* **66:** 486–501

Espeli O, Levine C, Hassing H, Marians KJ (2003) Temporal regulation of topoisomerase IV activity in E. coli. *Mol Cell* **11:** 189–201

Fachinetti D, Bermejo R, Cocito A, Minardi S, Katou Y, Kanoh Y, Shirahige K, Azvolinsky A, Zakian VA, Foiani M (2010) Replication termination at eukaryotic chromosomes is mediated by Top2 and occurs at genomic loci containing pausing elements. *Mol Cell* **39:** 595–605

Gellert M, Mizuuchi K, O'Dea MH, Nash HA (1976) DNA gyrase: an enzyme that introduces superhelical turns into DNA. *Proc Natl Acad Sci USA* **73:** 3872–3876

Graumann PL (2000) Bacillus subtilis SMC is required for proper arrangement of the chromosome and for efficient segregation of replication termini but not for bipolar movement of newly duplicated origin regions. *J Bacteriol* **182:** 6463–6471

Griese JJ, Hopfner KP (2010) Structure and DNA-binding activity of the Pyrococcus furiosus SMC protein hinge domain. *Proteins* **79:** 558–568

Griese JJ, Witte G, Hopfner KP (2010) Structure and DNA binding activity of the mouse condensin hinge domain highlight common and diverse features of SMC proteins. *Nucleic Acids Res* **38:** 3454–3465

Hardy CD, Crisona NJ, Stone MD, Cozzarelli NR (2004) Disentangling DNA during replication: a tale of two strands. *Philos Trans R Soc London [Biol]* **359:** 39–47

Hartwell LH, Weinert TA (1989) Checkpoints: controls that ensure the order of cell cycle events. *Science* **246:** 629–634

Hayama R, Bahng S, Karasu ME, Marians KJ (2013) The MukB-ParC interaction affects intramolecular, not intermolecular, activities of topoisomerase IV. *J Biol Chem* **288:** 7653–7661

Hayama R, Marians KJ (2010) Physical and functional interaction between the condensin MukB and the decatenase topoisomerase IV in Escherichia coli. *Proc Natl Acad Sci USA* **107:** 18826–18831

Hiasa H, DiGate RJ, Marians KJ (1994) Decatenating activity of Escherichia coli DNA gyrase and topoisomerases I and III during oriC and pBR322 DNA replication in vitro. *J Biol Chem* **269:** 2093–2099

Hiasa H, Marians KJ (1996) Two distinct modes of strand unlinking during θ-type DNA replication. *J Biol Chem* **271:** 21529

Hiraga S, Niki H, Ogura T, Ichinose C (1989) Chromosome partitioning in Escherichia coli: novel mutants producing anucleate cells. *J Bacteriol* **171:** 1496–1505

Hirano M, Hirano T (2002) Hinge-mediated dimerization of SMC protein is essential for its dynamic interaction with DNA. *EMBO J* **21:** 5733–5744

Hirano M, Hirano T (2006) Opening closed arms: long-distance activation of SMC ATPase by hinge-DNA interactions. *Mol Cell* **21:** 175–186

Hirano T (2012) Condensins: universal organizers of chromosomes with diverse functions. *Genes Dev* **26:** 1659–1678

Holton J, Alber T (2004) Automated protein crystal structure determination using ELVES. *Proc Natl Acad Sci USA* **101:** 1537–1542

Huang WM, Libbey JL, van der Hoeven P, Yu SX (1998) Bipolar localization of Bacillus subtilis topoisomerase IV, an enzyme required for chromosome segregation. *Proc Natl Acad Sci USA* **95:** 4652–4657

 ©2013 European Molecular Biology Organization

Joshi MC, Bourniquel A, Fisher J, Ho BT, Magnan D, Kleckner N, Bates D (2011) Escherichia coli sister chromosome separation includes an abrupt global transition with concomitant release of late-splitting intersister snaps. *Proc Natl Acad Sci USA* **108:** 2765–2770

Kato J, Nishimura Y, Imamura R, Niki H, Hiraga S, Suzuki H (1990) New topoisomerase essential for chromosome segregation in E. coli. *Cell* **63:** 393–404

Kato J, Nishimura Y, Yamada M, Suzuki H, Hirota Y (1988) Gene organization in the region containing a new gene involved in chromosome partition in Escherichia coli. *J Bacteriol* **170:** 3967–3977

Kato J, Suzuki H, Ikeda H (1992) Purification and characterization of DNA topoisomerase IV in Escherichia coli. *J Biol Chem* **267:** 25676–25684

Kenakin TP (1993) *Pharmacologic Analysis of Drug-Receptor Interaction*. 2nd edn. New York: Raven

Khodursky AB, Peter BJ, Schmid MB, DeRisi J, Botstein D, Brown PO, Cozzarelli NR (2000) Analysis of topoisomerase function in bacterial replication fork movement: use of DNA microarrays. *Proc Natl Acad Sci USA* **97:** 9419–9424

Kirchhausen T, Wang JC, Harrison SC (1985) DNA gyrase and its complexes with DNA: direct observation by electron microscopy. *Cell* **41:** 933–943

Ku B, Lim JH, Shin HC, Shin SY, Oh BH (2009) Crystal structure of the MukB hinge domain with coiled-coil stretches and its functional implications. *Proteins* **78:** 1483–1490

Lavasani LS, Hiasa H (2001) A ParE-ParC fusion protein is a functional topoisomerase. *Biochemistry* **40:** 8438–8443

Lesterlin C, Gigant E, Boccard F, Espeli O (2012) Sister chromatid interactions in bacteria revealed by a site-specific recombination assay. *EMBO J* **31:** 3468–3479

Li Y, Schoeffler AJ, Berger JM, Oakley MG (2010a) The crystal structure of the hinge domain of the Escherichia coli structural maintenance of chromosomes protein MukB. *J Mol Biol* **395:** 11–19

Li Y, Stewart NK, Berger AJ, Vos S, Schoeffler AJ, Berger JM, Chait BT, Oakley MG (2010b) Escherichia coli condensin MukB stimulates topoisomerase IV activity by a direct physical interaction. *Proc Natl Acad Sci USA* **107:** 18832–18837

Li Y, Weitzel CS, Arnold RJ, Oakley MG (2009) Identification of interacting regions within the coiled coil of the Escherichia coli structural maintenance of chromosomes protein MukB. *J Mol Biol* **391:** 57–73

Lopez CR, Yang S, Deibler RW, Ray SA, Pennington JM, Digate RJ, Hastings PJ, Rosenberg SM, Zechiedrich EL (2005) A role for topoisomerase III in a recombination pathway alternative to RuvABC. *Mol Microbiol* **58:** 80–101

Luijsterburg MS, White MF, van Driel R, Dame RT (2008) The major architects of chromatin: architectural proteins in Bacteria, Archaea and Eukaryotes. *Crit Rev Biochem Mol Biol* **43:** 393–418

Lundblad JR, Laurance M, Goodman RH (1996) Fluorescence polarization analysis of protein-DNA and protein-protein interactions. *Mol Endocrinol* **10:** 607–612

MacDowell AA, Celestre RS, Howells M, McKinney W, Krupnick J, Cambie D, Domning EE, Duarte RM, Kelez N, Plate DW, Cork CW, Earnest TN, Dickert J, Meigs G, Ralston C, Holton JM, Alber T, Berger JM, Agard DA, Padmore HA (2004) Suite of three protein crystallography beamlines with single superconducting bend magnet as the source. *J Synchrotron Radiat* **11:** 447–455

Melby TE, Ciampaglio CN, Briscoe G, Erickson HP (1998) The symmetrical structure of structural maintenance of chromosomes (SMC) and MukB proteins: long, antiparallel coiled coils, folded at a flexible hinge. *J Cell Biol* **142:** 1595–1604

Neuman KC, Charvin G, Bensimon D, Croquette V (2009) Mechanisms of chiral discrimination by topoisomerase IV. *Proc Natl Acad Sci USA* **106:** 6986–6991

Nielsen HJ, Li Y, Youngren B, Hansen FG, Austin S (2006) Progressive segregation of the Escherichia coli chromosome. *Mol Microbiol* **61:** 383–393

Niki H, Jaffé A, Imamura R, Ogura T, Hiraga S (1991) The new gene mukB codes for a 177 kd protein with coiled-coil domains involved in chromosome partitioning of E. coli. *EMBO J* **10:** 183–193

Nurse P, Levine C, Hassing H, Marians KJ (2003) Topoisomerase III can serve as the cellular decatenase in Escherichia coli. *J Biol Chem* **278:** 8653–8660

Otwinowski Z, Minor W (1997) Processing of X-ray diffraction data collected in oscillation mode. In *Methods in Enzymology. Macromolecular Crystallography, part A*, SR Carter CW (ed), Vol. 276, pp 307–326. New York: Academic Press

Painter J, Merritt E (2006) TLSMD web server for the generation of multi-group TLS models. *J Appl Cryst* **39:** 109–111

Papillon J, Menetret JF, Batisse C, Helye R, Schultz P, Potier N, Lamour V (2013) Structural insight into negative DNA supercoiling by DNA gyrase, a bacterial type 2A DNA topoisomerase. *Nucleic Acids Res* **41:** 7815–7827

Peng H, Marians KJ (1993a) Decatenation activity of topoisomerase IV during oriC and pBR322 DNA replication *in vitro*. *Proc Natl Acad Sci USA* **90:** 8571–8575

Peng H, Marians KJ (1993b) Escherichia coli topoisomerase IV. Purification, characterization, subunit structure, and subunit interactions. *J Biol Chem* **268:** 24481–24490

Perez-Cheeks BA, Lee C, Hayama R, Marians KJ (2012) A role for topoisomerase III in Escherichia coli chromosome segregation. *Mol Microbiol* **86:** 1007–1022

Peter BJ, Ullsperger C, Hiasa H, Marians KJ, Cozzarelli NR (1998) The structure of supercoiled intermediates in DNA replication. *Cell* **94:** 819–827

Petrushenko ZM, Cui Y, She W, Rybenkov VV (2010) Mechanics of DNA bridging by bacterial condensin MukBEF *in vitro* and in singulo. *EMBO J* **29:** 1126–1135

Petrushenko ZM, Lai CH, Rai R, Rybenkov VV (2006a) DNA reshaping by MukB. Right-handed knotting, left-handed supercoiling. *J Biol Chem* **281:** 4606–4615

Petrushenko ZM, Lai CH, Rybenkov VV (2006b) Antagonistic interactions of kleisins and DNA with bacterial Condensin MukB. *J Biol Chem* **281:** 34208–34217

Postow L, Crisona NJ, Peter BJ, Hardy CD, Cozzarelli NR (2001a) Topological challenges to DNA replication: conformations at the fork. *Proc Natl Acad Sci USA* **98:** 8219–8226

Postow L, Hardy CD, Arsuaga J, Cozzarelli NR (2004) Topological domain structure of the Escherichia coli chromosome. *Gene Dev* **18:** 1766–1779

Postow L, Ullsperger C, Keller RW, Bustamante C, Vologodskii AV, Cozzarelli NR (2001b) Positive torsional strain causes the formation of a four-way junction at replication forks. *J Biol Chem* **276:** 2790–2796

Reece RJ, Maxwell A (1991) The C-terminal domain of the Escherichia coli DNA gyrase A subunit is a DNA-binding protein. *Nucleic Acids Res* **19:** 1399–1405

Reyes-Lamothe R, Possoz C, Danilova O, Sherratt DJ (2008) Independent positioning and action of Escherichia coli replisomes in live cells. *Cell* **133:** 90–102

Rodriguez AC (2002) Studies of a positive supercoiling machine. Nucleotide hydrolysis and a multifunctional 'latch' in the mechanism of reverse gyrase. *J Biol Chem* **277:** 29865–29873

Ruthenburg AJ, Graybosch DM, Huetsch JC, Verdine GL (2005) A superhelical spiral in the Escherichia coli DNA gyrase A C-terminal domain imparts unidirectional supercoiling bias. *J Biol Chem* **280:** 26177–26184

Sambrook J, Russell DW (2001) *Molecular Cloning: A Laboratory Manual*. 3rd edn. Cold Spring Harbor, New York: CSHL Press

Schmidt BH, Osheroff N, Berger JM (2012) Structure of a topoisomerase II-DNA-nucleotide complex reveals a new control mechanism for ATPase activity. *Nat Struct Mol Biol* **19:** 1147–1154

She W, Wang Q, Mordukhova EA, Rybenkov VV (2007) MukEF Is required for stable association of MukB with the chromosome. *J Bacteriol* **189:** 7062–7068

Sogo JM, Stasiak A, Martínez-Robles ML, Krimer DB, Hernández P, Schvartzman JB (1999) Formation of knots in partially replicated DNA molecules. *J Mol Biol* **286:** 637–643

Stone MD, Bryant Z, Crisona NJ, Smith SB, Vologodskii A, Bustamante C, Cozzarelli NR (2003) Chirality sensing by Escherichia coli topoisomerase IV and the mechanism of type II topoisomerases. *Proc Natl Acad Sci USA* **100:** 8654–8659

Sunako Y, Onogi T, Hiraga S (2001) Sister chromosome cohesion of Escherichia coli. *Mol Microbiol* **42:** 1233–1241

Swillens S (1995) Interpretation of binding curves obtained with high receptor concentrations: practical aid for computer analysis. *Mol Pharmacol* **47:** 1197–1203

©2013 European Molecular Biology Organization

Taniguchi Y, Choi PJ, Li GW, Chen H, Babu M, Hearn J, Emili A, Xie XS (2010) Quantifying E. coli proteome and transcriptome with single-molecule sensitivity in single cells. *Science* **329:** 533–538

Terwilliger TC, Adams PD, Read RJ, McCoy AJ, Moriarty NW, Grosse-Kunstleve RW, Afonine PV, Zwart PH, Hung LW (2009) Decision-making in structure solution using Bayesian estimates of map quality: the PHENIX AutoSol wizard. *Acta Crystallogr D Biol Crystallogr* **65:** 582–601

Tretter EM, Berger JM (2012) Mechanisms for Defining Supercoiling Set Point of DNA Gyrase Orthologs: I. A NONCONSERVED ACIDIC C-TERMINAL TAIL MODULATES ESCHERICHIA COLI GYRASE ACTIVITY. *J Biol Chem* **287:** 18636–18644

Uhlmann F, Nasmyth K (1998) Cohesion between sister chromatids must be established during DNA replication. *Curr Biol* **8:** 1095–1101

Van Duyne G, Standaert R, Karplus P, Schreiber S, Clardy J (1993) Atomic structures of the human immunophilin FKBP-12 complexes with FK506 and rapamycin. *J Mol Biol* **229:** 105–124

Viollier PH, Thanbichler M, McGrath PT, West L, Meewan M, McAdams HH, Shapiro L (2004) Rapid and sequential movement of individual chromosomal loci to specific subcellular locations during bacterial DNA replication. *Proc Natl Acad Sci USA* **101:** 9257–9262

Vos SM, Lee I, Berger JM (2013) Distinct regions of the *Escherchia coli* Par C C-terminal domain are required for substrate discrimination by topoisomerase IV. *J Mol Biol* **425:** 3029–3045

Wang M, Weiss M, Simonovic M, Haertinger G, Schrimpf SP, Hengartner MO, von Mering C (2012) PaxDb, a database of protein abundance averages across all three domains of life. *Mol Cell Proteomics* **11:** 492–500

Wang Q, Mordukhova EA, Edwards AL, Rybenkov VV (2006a) Chromosome condensation in the absence of the non-SMC subunits of MukBEF. *J Bacteriol* **188:** 4431–4441

Wang SC, Shapiro L (2004) The topoisomerase IV ParC subunit colocalizes with the Caulobacter replisome and is required for polar localization of replication origins. *Proc Natl Acad Sci USA* **101:** 9251–9256

Wang X, Liu X, Possoz C, Sherratt DJ (2006b) The two Escherichia coli chromosome arms locate to separate cell halves. *Genes Dev* **20:** 1727–1731

Wang X, Reyes-Lamothe R, Sherratt DJ (2008) Modulation of Escherichia coli sister chromosome cohesion by topoisomerase IV. *Genes Dev* **22:** 2426–2433

Weinert TA, Kiser GL, Hartwell LH (1994) Mitotic checkpoint genes in budding yeast and the dependence of mitosis on DNA replication and repair. *Genes Dev* **8:** 652–665

Woo JS, Lim JH, Shin HC, Suh MK, Ku B, Lee KH, Joo K, Robinson H, Lee J, Park SY, Ha NC, Oh BH (2009) Structural studies of a bacterial condensin complex reveal ATP-dependent disruption of intersubunit interactions. *Cell* **136:** 85–96

Zechiedrich E, Cozzarelli N (1995) Roles of topoisomerase IV and DNA gyrase in DNA unlinking during replication in Escherichia coli. *Genes Dev* **9:** 2859

 ©2013 European Molecular Biology Organization